Supporting Materials

Fast Accessing the Lattice Thermal Conductivity and Phonon Quasiparticle Spectra of $Mo_2TiC_2T_2$ (T = -O and -F) and Janus Mo_2TiC_2OF MXenes from Machine Learning Potentials

Yiding Qiu, Ziang Jing, Haoliang Liu, Huaxuan He, KaiWu, Yonghong Cheng, Bing Xiao*

School of Electrical Engineering, State Key Laboratory of Electrical Insulation and Power Equipment, Xi'an Jiaotong University, Xi'an Shaanxi, 710049, P.R. China

*Correspondence Author: bingxiao84@xjtu.edu.cn

Table S1 The equilibrium energies (eV) of Mo_2TiC_2 and $Mo_2TiC_2T_2$ (T = -O and -F) and Janus Mo_2TiC_2OF MXenes.

Mo_2TiC_2	-47.6	
	AA	BB
$Mo_2TiC_2O_2$	-65.2	-64.1
$Mo_2TiC_2F_2$	-58.6	-58.5
Mo_2TiC_2OF	-61.9	-61.3

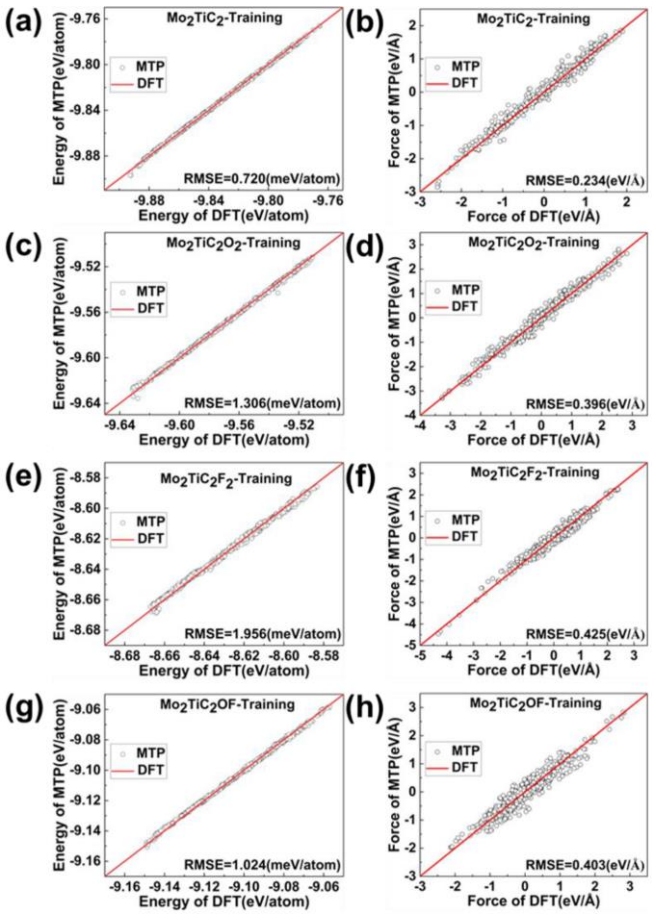

Fig. S1 Comparison of total energies and atomic forces between MTP and DFT calculations for training datasets: (a)-(b): Mo_2TiC_2; (c)-(d): $Mo_2TiC_2O_2$; (e)-(f): $Mo_2TiC_2F_2$; (g)-(h): Janus-Mo_2TiC_2OF.

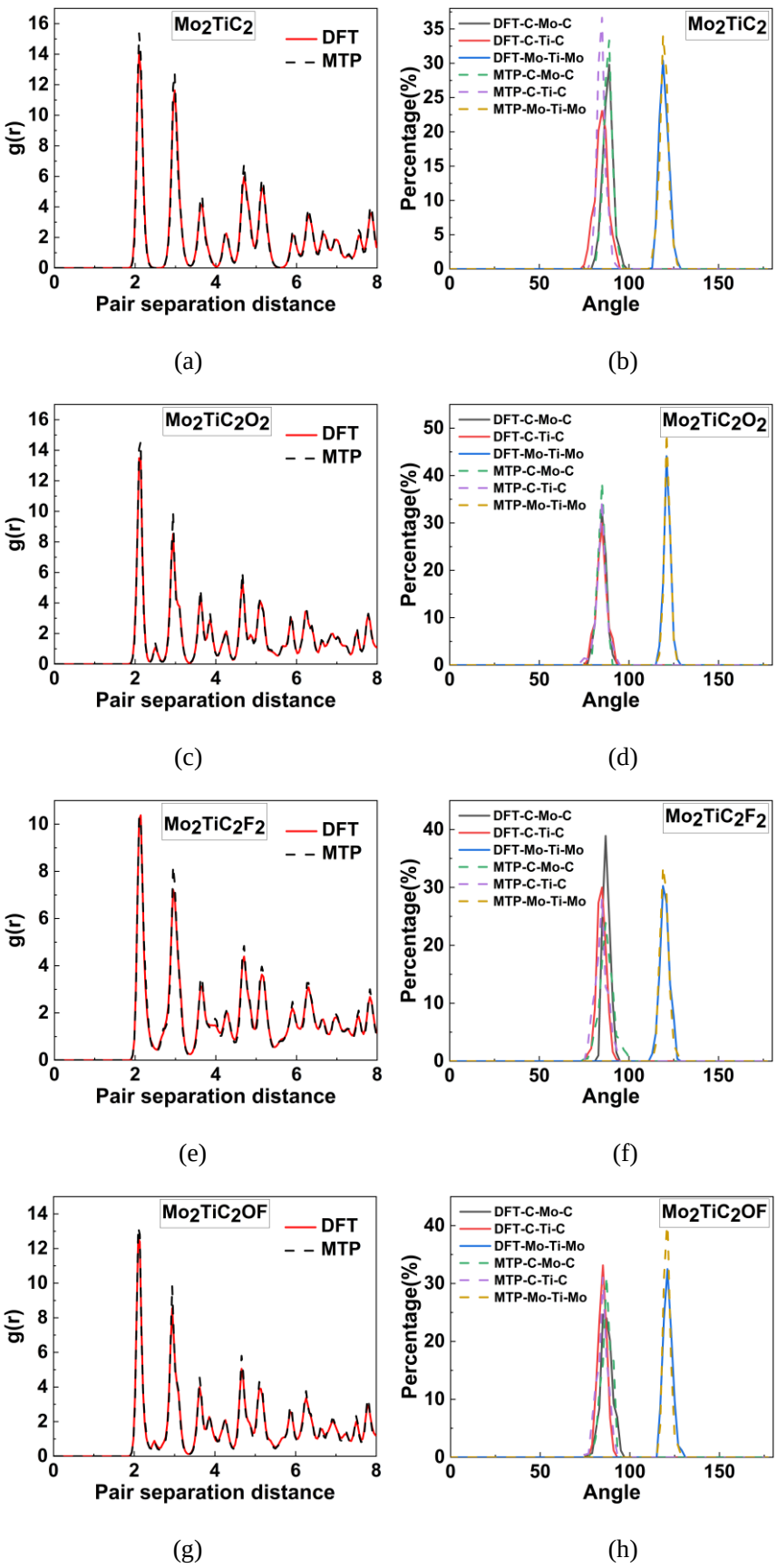

Fig. S2 Comparison of total radial distribution function (RDF) and bond angle distribution function (ADF) between MTP and DFT calculations for MXenes: (a-b): Mo_2TiC_2; (c-d): $Mo_2TiC_2O_2$; (e-f): $Mo_2TiC_2F_2$; (g-h): Janus-Mo_2TiC_2OF.

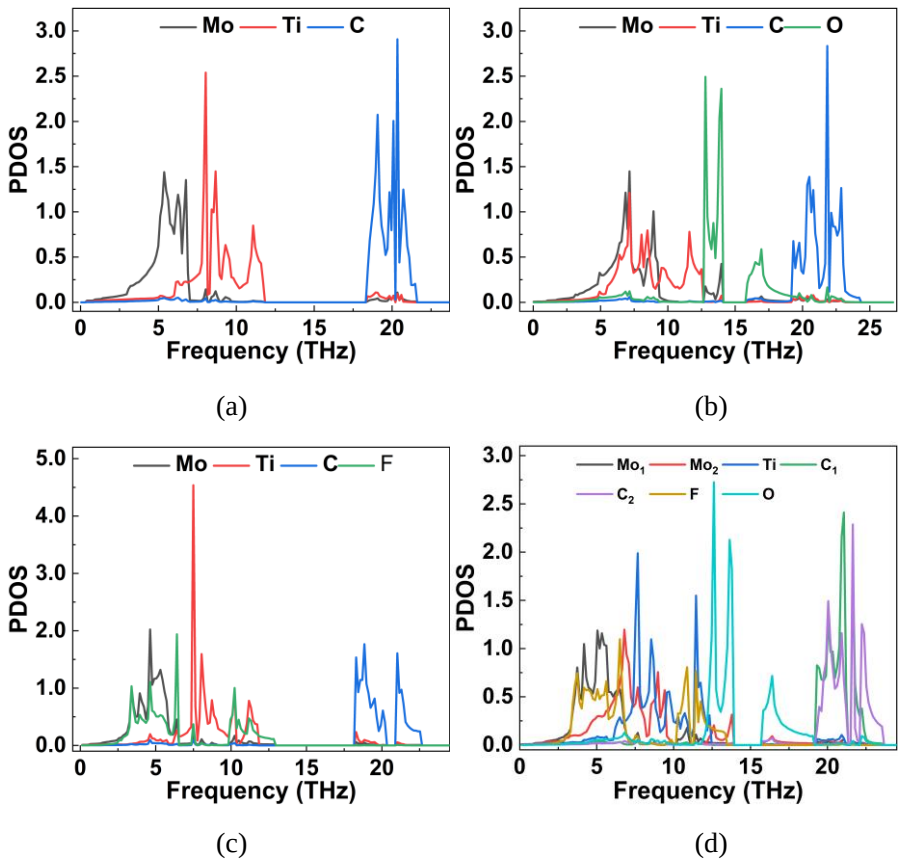

Fig. S3 Atomic species resolved phonon density of states obtained using MTPs: (a): Mo_2TiC_2; (b): $Mo_2TiC_2O_2$; (c): $Mo_2TiC_2F_2$; (d): Janus-Mo_2TiC_2OF.

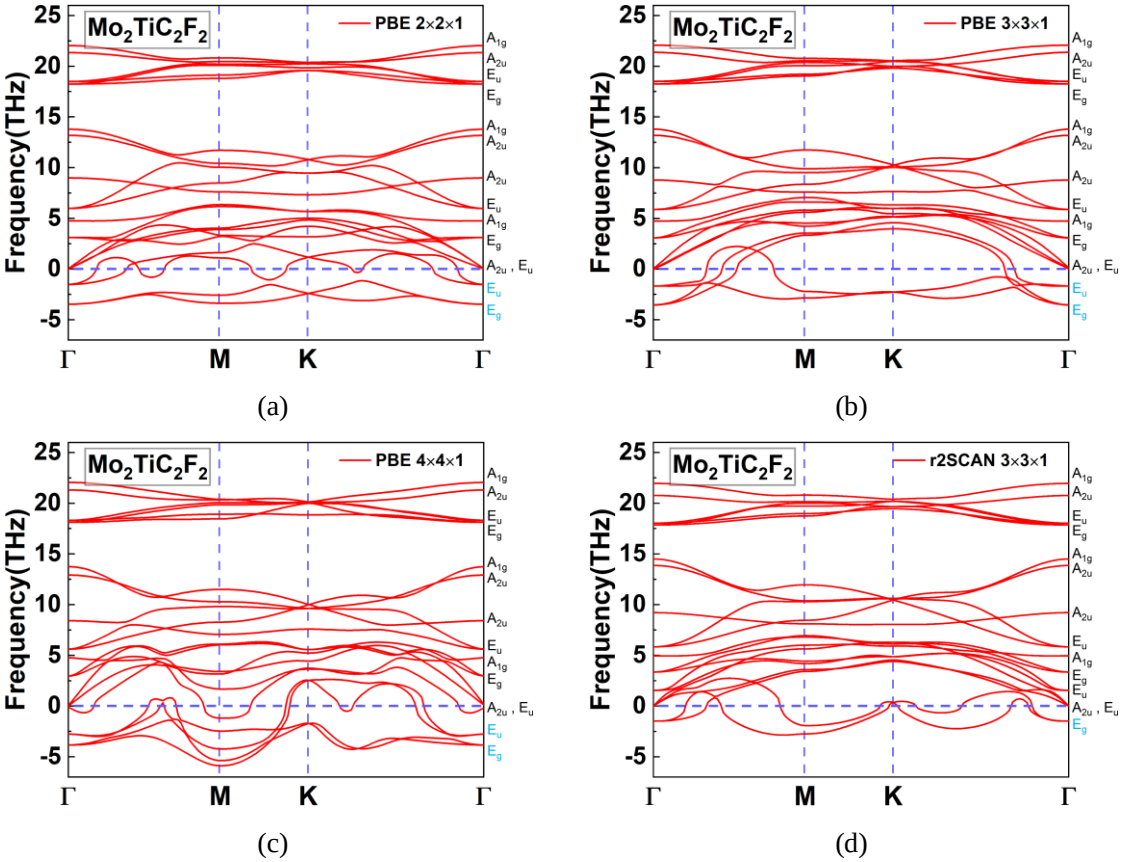

Fig. S4 The harmonic phonon dispersions of $Mo_2TiC_2F_2$ calculated by different functionals with various k-points mesh: PBE functional: (a) 2×2×1; (b) 3×3×1; (c) 4×4×1; r^2SCAN: (d) 3×3×1).

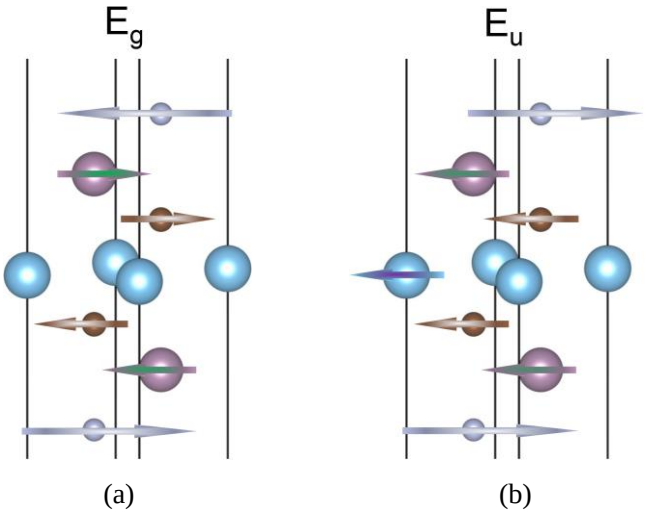

Fig. S5 The phonon vibration eigenvectors with imaginary frequency at Gamma point (Γ(0, 0,0)) of $Mo_2TiC_2F_2$. The length of the arrow represents the amplitude of the specific atom vibrations.

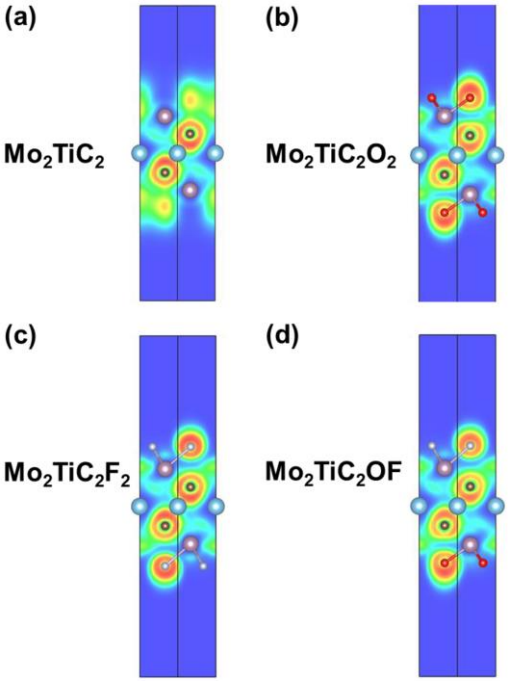

Fig. S6: The electron localization function (ELF) of MXenes: (a) Mo_2TiC_2; (b) $Mo_2TiC_2O_2$; (c) $Mo_2TiC_2F_2$; (d) Mo_2TiC_2OF.

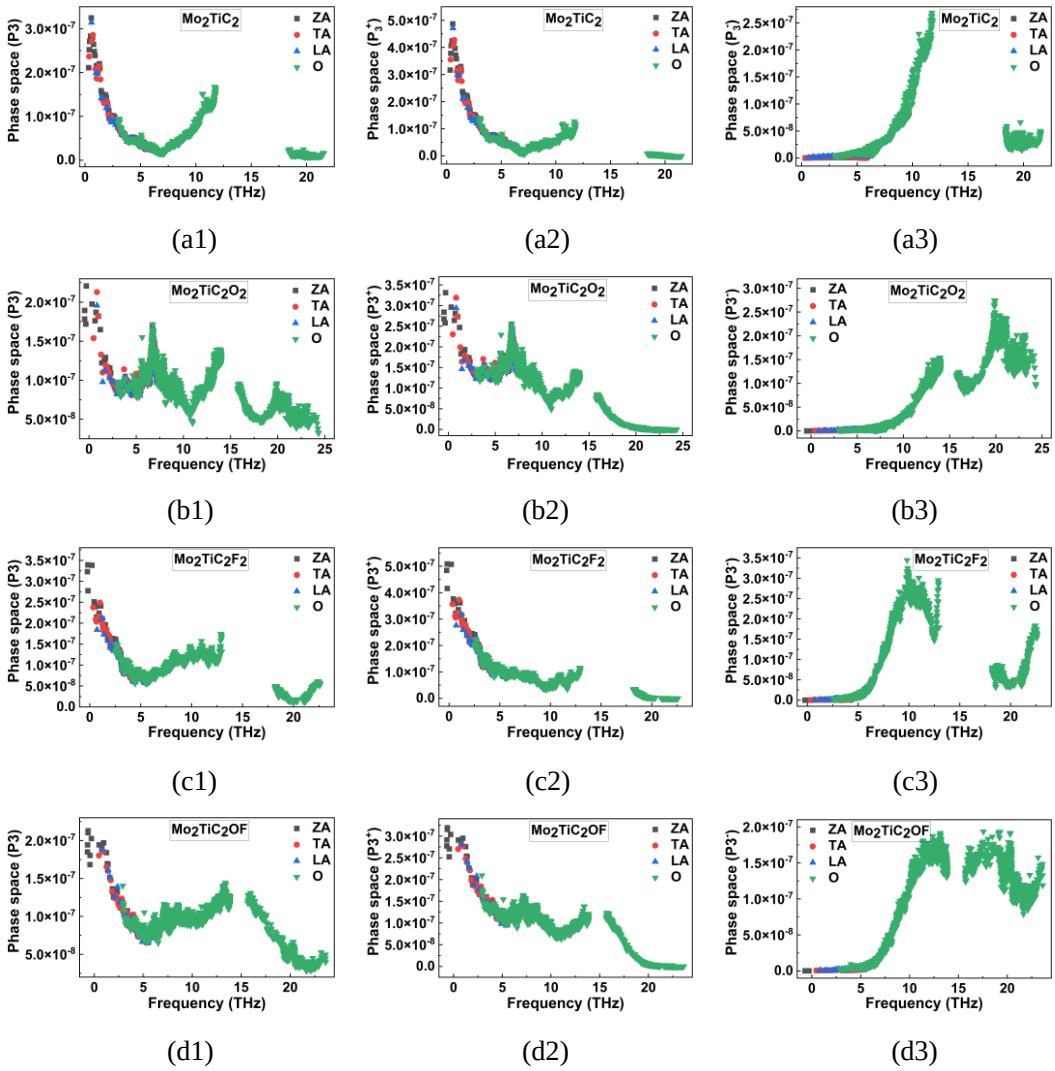

Fig. S7 Mode resolved three-phonon scattering phase space diagrams of MXenes including the total three-phonon scattering space, the combination process and the splitting process: (a1)-(a3): Mo_2TiC_2; (b1)-(b3): $Mo_2TiC_2O_2$; (c1)-(c3): $Mo_2TiC_2F_2$; (d1)-(d3): Janus-Mo_2TiC_2OF. ZA: the out-of-plane flexural mode; LA and TA: the in-plane longitudinal and transverse acoustic modes; O: optical modes.

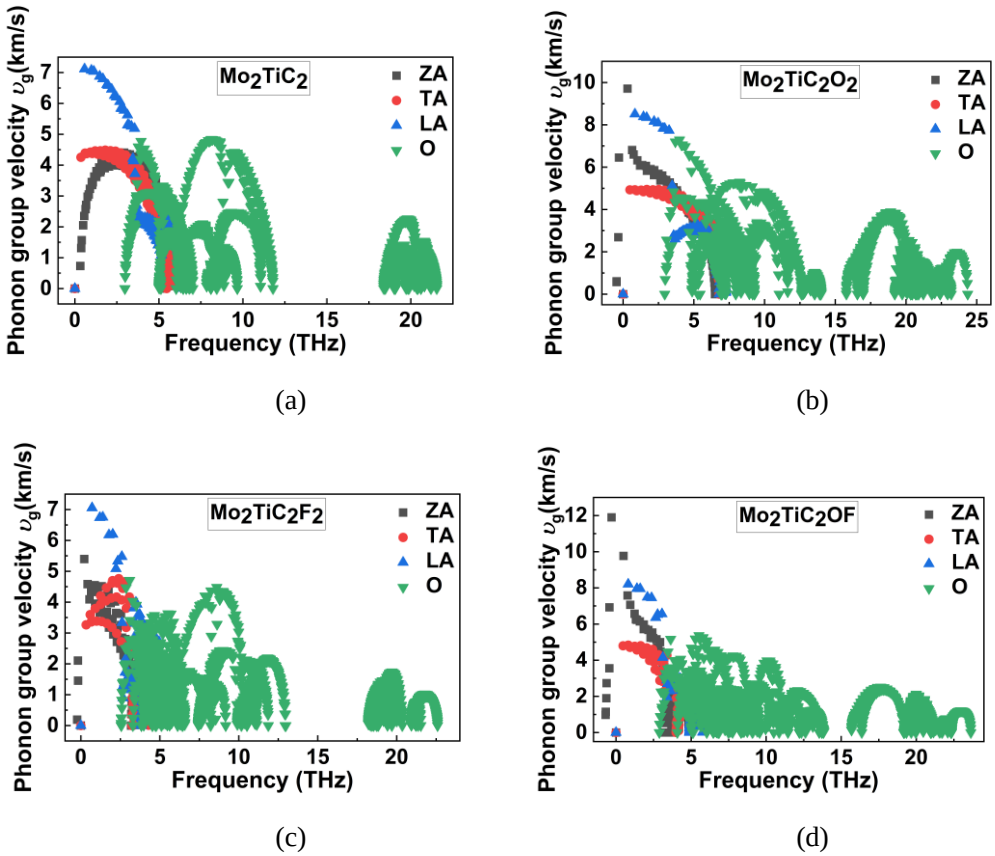

Fig. S8 Mode-resolved phonon group velocities at room temperature (300 K) for MXenes: (a): Mo_2TiC_2; (b): $Mo_2TiC_2O_2$; (c): $Mo_2TiC_2F_2$; (d): Janus-Mo_2TiC_2OF. ZA: out-of-plane flexural mode; TA: in-plane transverse acoustic mode; LA: in-plane longitudinal acoustic mode; O: optical branches.

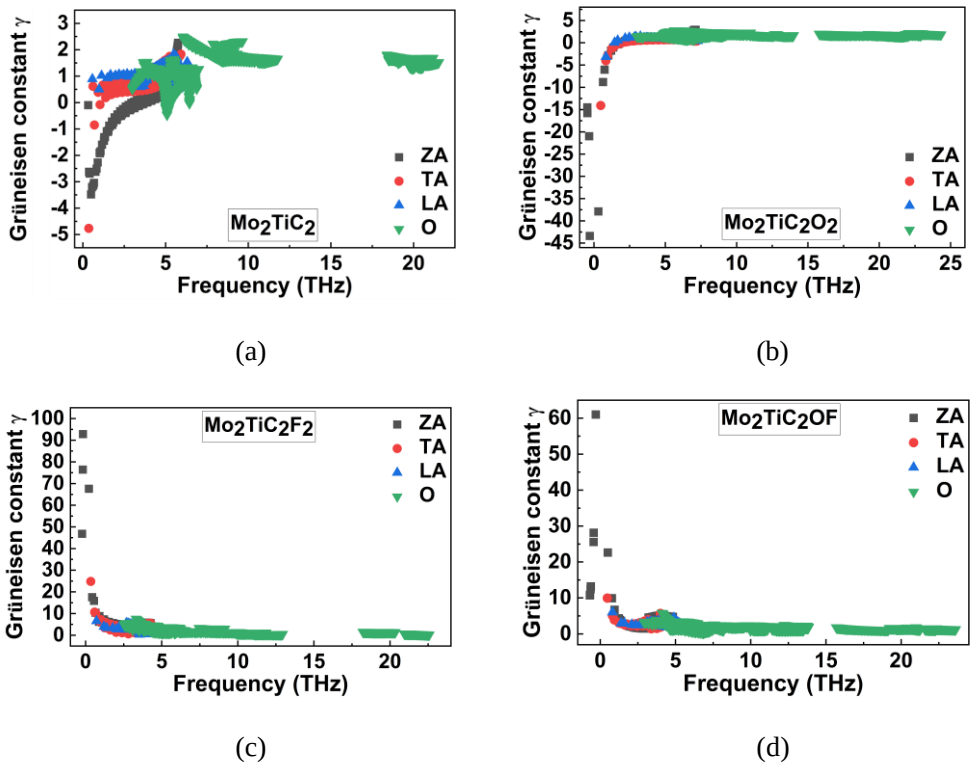

Fig. S9 Mode-Grüneisen parameters obtained from MTPs for MXenes: (a) Mo_2TiC_2; (b) $Mo_2TiC_2O_2$; (c) $Mo_2TiC_2F_2$; (d) Janus-Mo_2TiC_2OF.

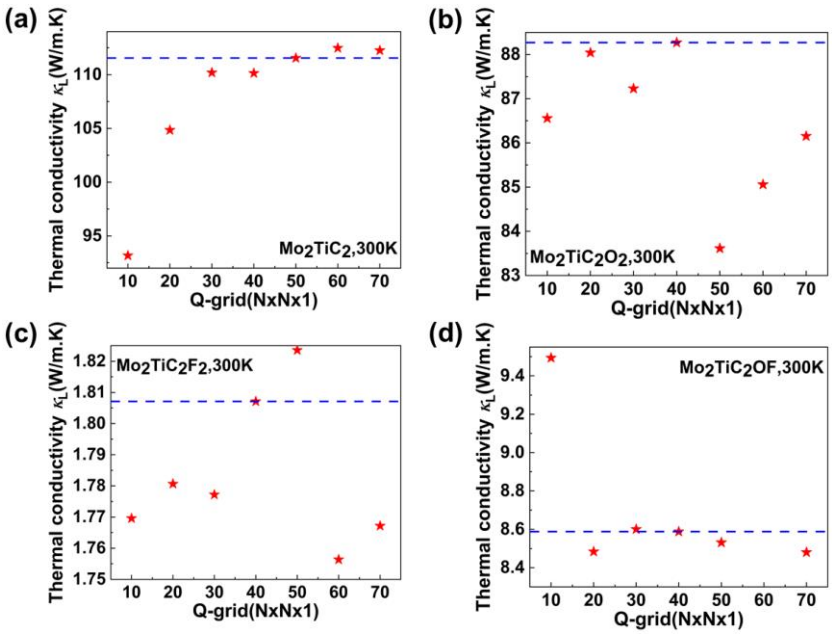

Fig. S10: The lattice thermal conductivity of MXenes converges with Q-grid: (a) Mo_2TiC_2; (b) $Mo_2TiC_2O_2$; (c) $Mo_2TiC_2F_2$; (d) Mo_2TiC_2OF.

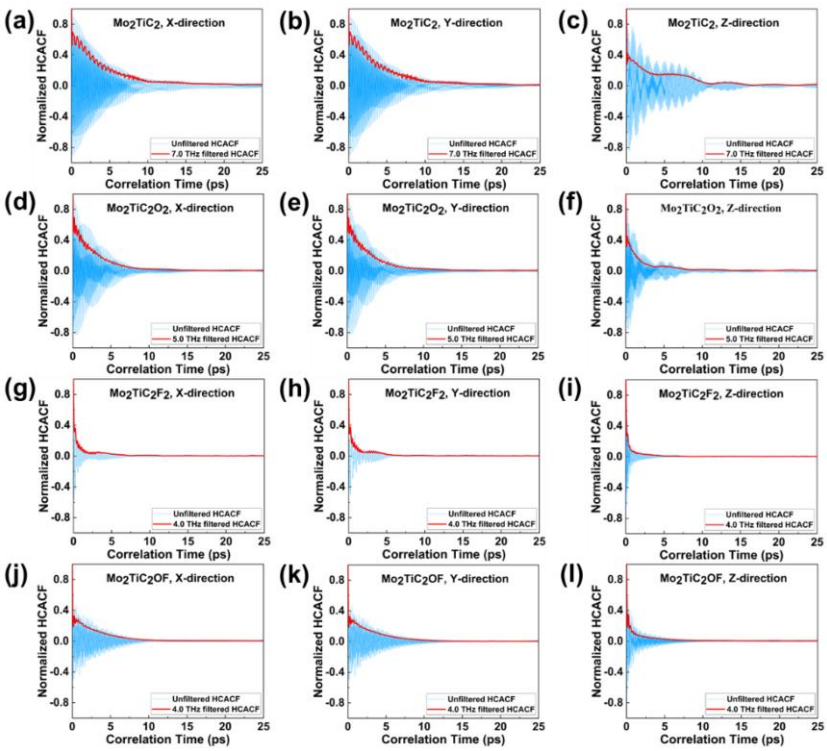

Fig. S11 Unfiltered and filtered normalized HCACF with correlation time: (a-c) Mo_2TiC_2; (d-f) $Mo_2TiC_2O_2$; (g-i) $Mo_2TiC_2F_2$; (j-l) Mo_2TiC_2OF.

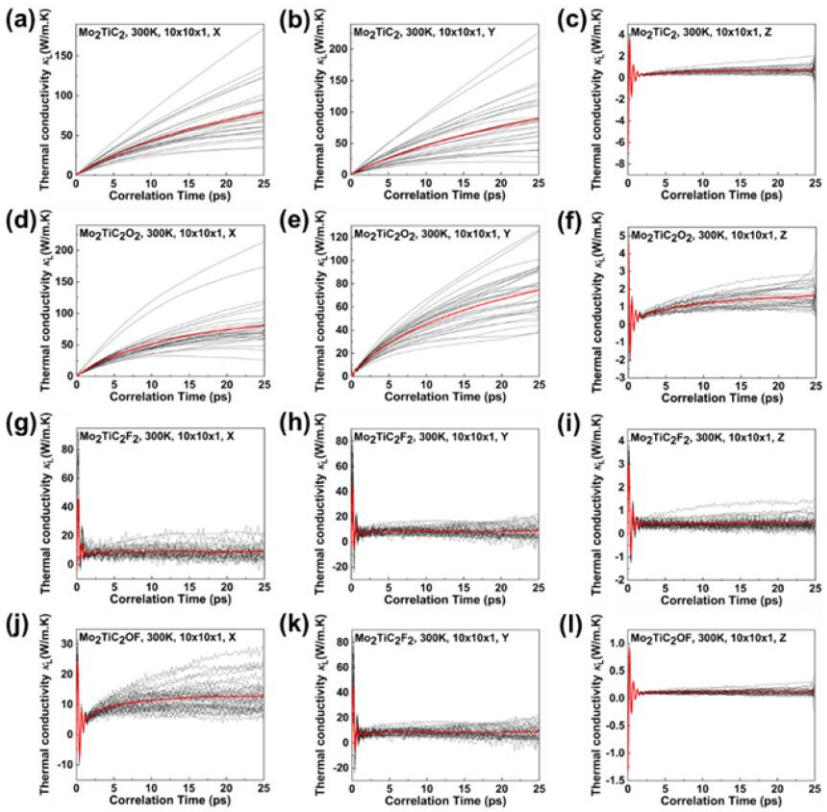

Fig. S12: Thermal conductivities along the x, y, and z directions with correlation time (a-c) Mo_2TiC_2; (d-f) $Mo_2TiC_2O_2$; (g-i) $Mo_2TiC_2F_2$; (j-l) Mo_2TiC_2OF.

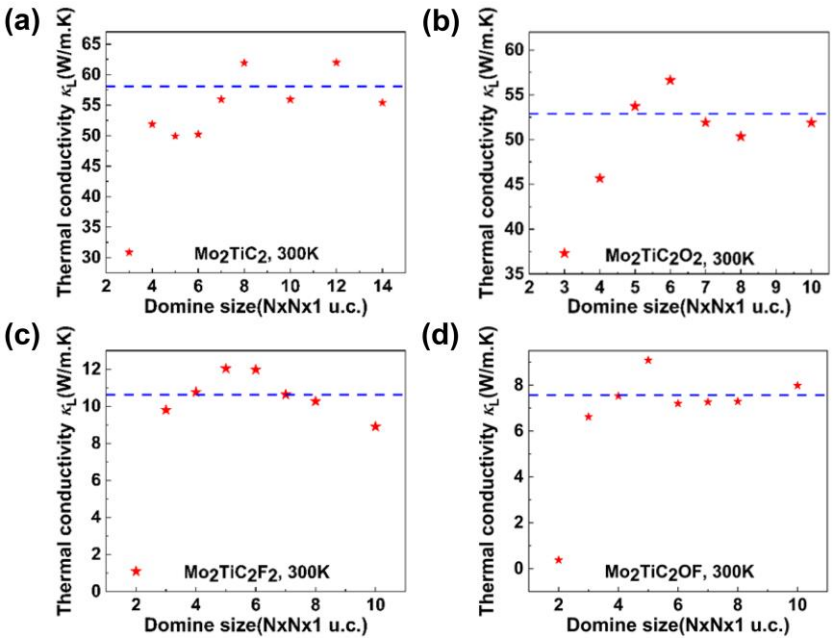

Fig. S13: The EMD method predicts the thermal conductivity of MXenes at 300K with the size of the simulation domain: (a) Mo_2TiC_2; (b) $Mo_2TiC_2O_2$; (c) $Mo_2TiC_2F_2$; (d) Mo_2TiC_2OF.

Spectral Energy Density

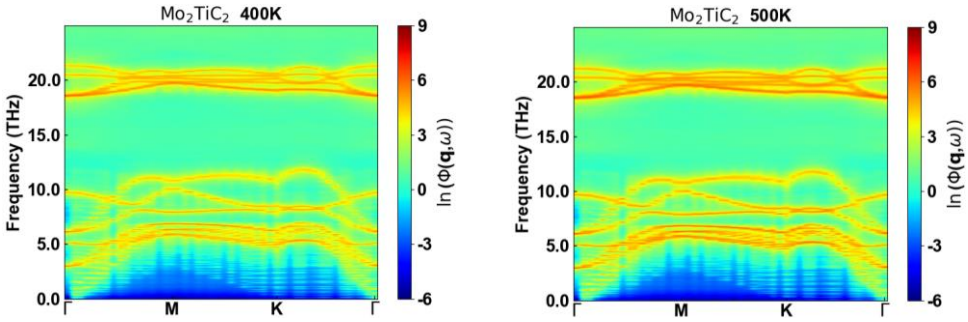

(a) (b)

Fig. S14 Phonon quasi-particle spectral energy density of Mo_2TiC_2 monolayer obtained from classic molecular dynamics simulations using MTP: (a): 400 K; (b): 500 K.

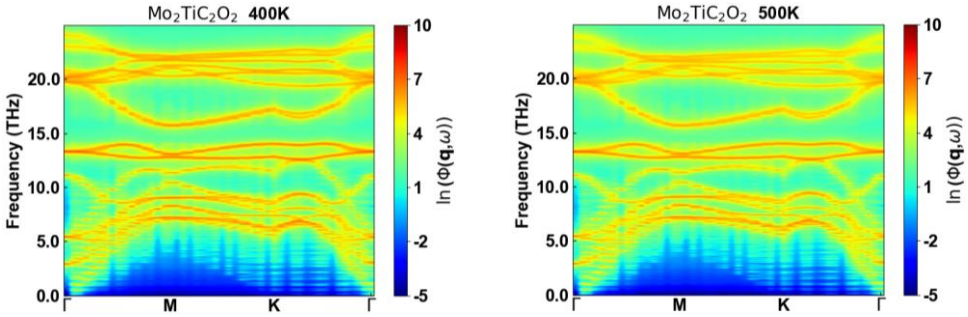

(a) (b)

Fig. S15 Phonon quasi-particle spectral energy density of $Mo_2TiC_2O_2$ monolayer obtained from classic molecular dynamics simulations using MTP: (a): 400 K; (b): 500 K.

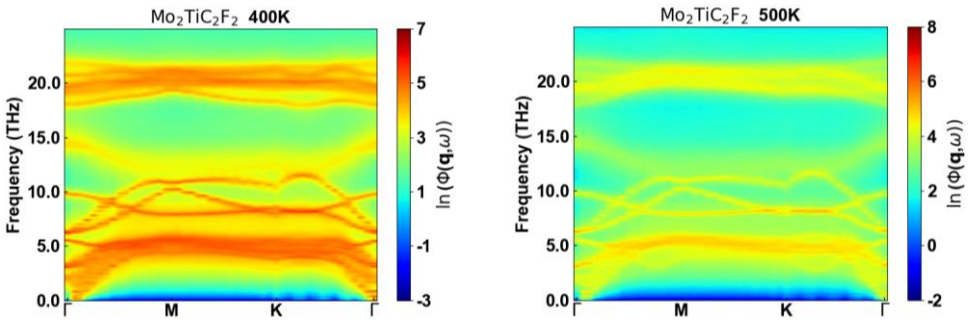

(a) (b)

Fig. S16 Phonon quasi-particle spectral energy density of $Mo_2TiC_2F_2$ monolayer obtained from classic molecular dynamics simulations using MTP: (a): 400 K; (b): 500 K.

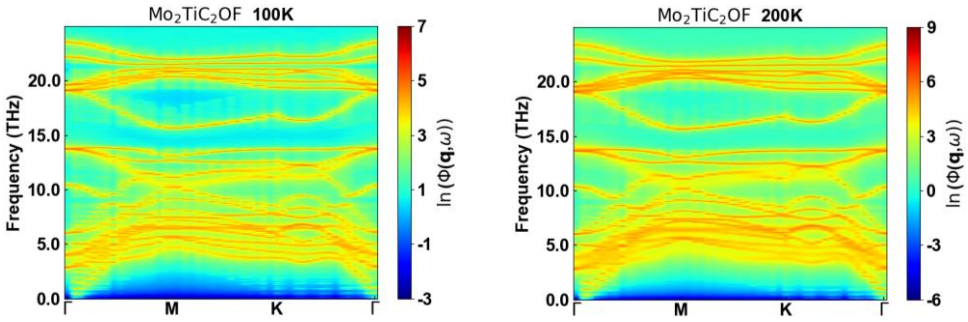

(a) (b)

Fig. S17 Phonon quasi-particle spectral energy density of Janus-Mo_2TiC_2OF monolayer obtained from classic molecular dynamics simulations using MTP: (a): 100 K; (b): 200 K.

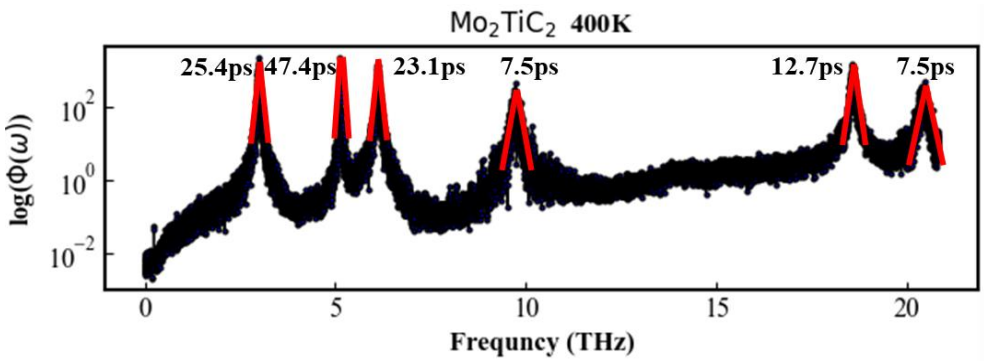

(a)

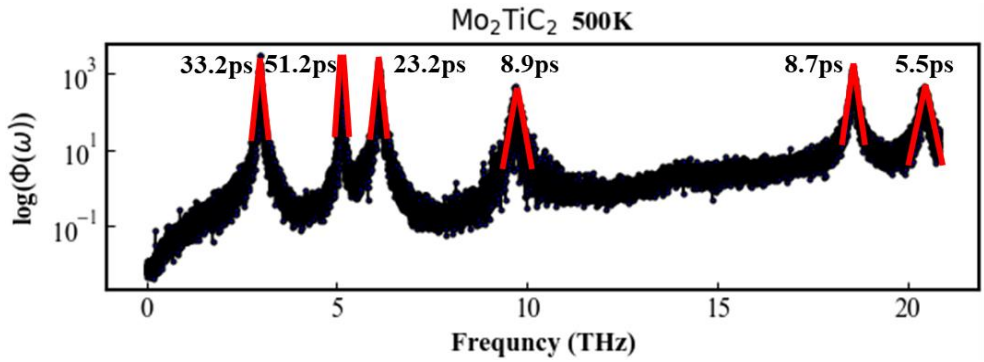

(b)

Fig. S18 Phonon quasi-particle spectral energy density of Mo_2TiC_2 monolayer at Γ-point in the Brillouin zone obtained from classic molecular dynamics simulations using MTP: (a): 400 K; (b): 500 K.

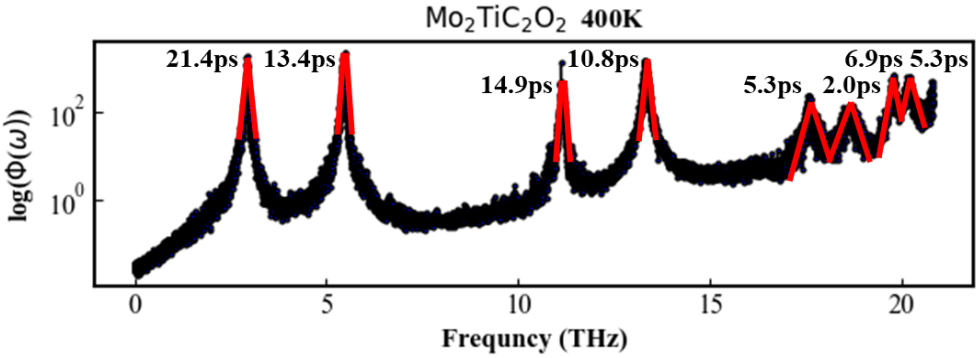

(a)

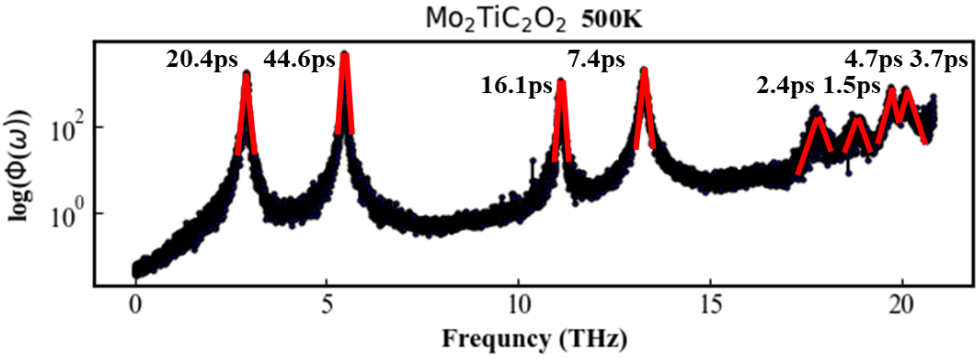

(b)

Fig. S19 Phonon quasi-particle spectral energy density of $Mo_2TiC_2O_2$ monolayer at Γ-point in the Brillouin zone obtained from classic molecular dynamics simulations using MTP: (a): 400 K; (b): 500 K.

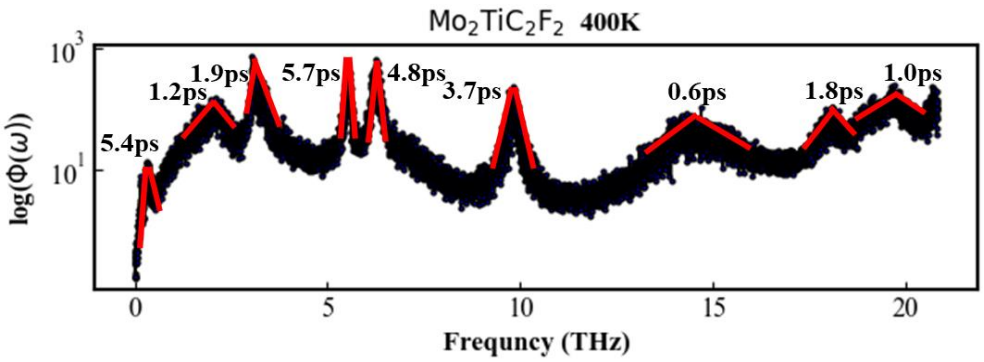

(a)

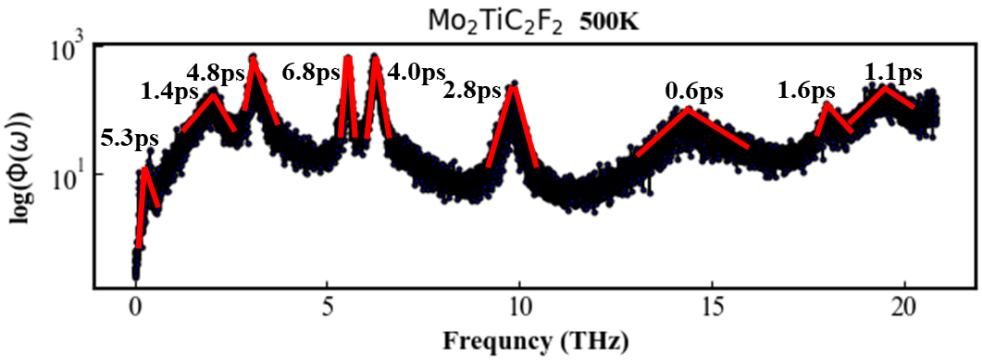

(b)

Fig. S20 Phonon quasi-particle spectral energy density of $Mo_2TiC_2F_2$ monolayer at Γ-point in the Brillouin zone obtained from classic molecular dynamics simulations using MTP: (a): 400 K; (b): 500 K.

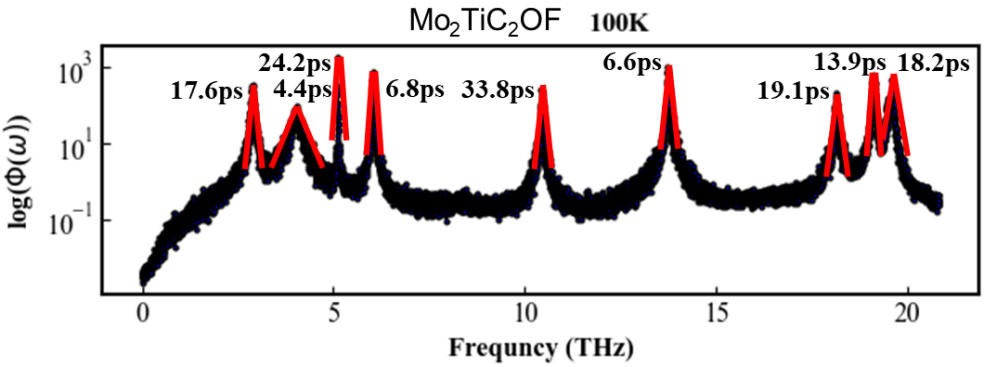

(a)

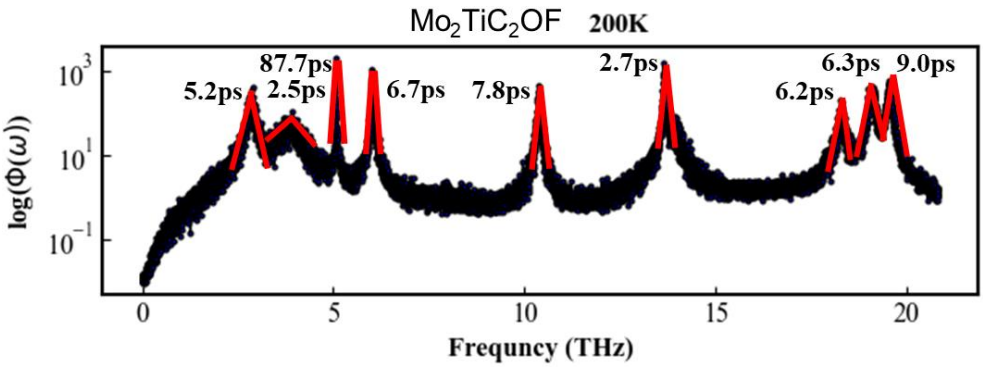

(b)

Fig. S21 Phonon quasi-particle spectral energy density of Janus-Mo_2TiC_2OF monolayer at Γ-point in the Brillouin zone obtained from classic molecular dynamics simulations using MTP: (a): 100 K; (b): 200 K.